II. EXPERIMENTAL FACILITIES

High performance of Temperature Gradient Chamber and CO_2-Temperature Gradient Chamber newly built for studying global warming effect on a plant and plant population

II-1. MATERIALS AND METHODS

II-1-1. Chamber design

Field facilities for studying the effects of global warming on plant growth were built at the Terrestrial Environment Research Center at the University of Tsukuba (36 06' 35" N, 140 06' 00" E, 27 m above sea level), Japan, in 1996-1997 (cf. Fig. 1). The annual precipitation in this area is 1,300 mm, and the annual mean temperature is 14℃.

Long sides of both the chambers were along the direction of North-East 35 . They were constructed 2.5-m high, 3-m wide and 30-m long using a commercial free-standing greenhouse tunnel. Their framework consisted of a series of semi-circular support pipes connected by pipe joints (ϕ 22.1 mm) coated with zinc. (Taiyou Kogyou. Tokyo, Japan; see Table 1 for list of equipment and vendors). Both ends of the pipes (0.3 m long) were anchored in to the ground. A ridge pipe running perpendicular to the support pipes anchored the pipes together at 0.5 m intervals. The frameworks were covered with 0.15 mm thick UV-transparent polyvinyl films (Super Solar Muteki, Mitsubishi, Tokyo, Japan; Table 1) that have a transparency of 65-87% to wavelengths of 250-700 nm. The films were fixed on the frameworks with metal fittings, and the ends were buried in the soil. To prevent ambient air transparency due to deposition of dusts, the outer surface of the film was cleaned with a sponge brush once every month.

The wall of the cool end of each chamber was covered with porous

Figure 1. Photographs of Control Chamber (CC, right top of photograph a), Temperature Gradient Chamber (TGC) with ambient CO_2 type (right top of photograph a), and the CO_2-Temperature Gradient Chamber (CTGC) with CO_2 enrichment type (right bottom of photograph a). Photograph (b) showing the inside of the CTGC.

Table 1. Materials and equipments and their suppliers

Materials/ equipment	Makers/ models	Suppliers (Japan)
Chamber frameworks steel pipe & joint parts	22.1 mm Galvanized	Taiyo Kogyo Co., Tokyo
PVC films	Super solar muteki	Mitsubishi Chemical Co., Tokyo
Ventilators	FKVP404203, 60607	Fulta Electric Co., Tokyo
Copper-Constantan wires	0.3 mm	Ninomiya Densen In. Co., Tokyo
Inverters	A024, A044	Mitsubishi Electric Co., Tokyo
Pyranometers	MS-42	EKO Co., Tokyo
Oil heaters	EH-50N	Ennez Co., Gunma, Tokyo
Electronic mass-flow controller (CO_2 gas supply)	PI-D1-1	CKD Co., Nagoya, Tokyo
Gas heater & flow-direction changer	ATM-2A(AC200V)	Yutaka Ltd., Tokyo
CO_2 analyzer	LI-6262	LI-Cor., Lincoln, USA
	ZFU	Fuji Electric Co., Tokyo
Blowers	BLW100-401	Fulta Electric Co., Tokyo
Data logger	Green Kit 100	ESD Co., Tokyo
Software for data logger	DL300	ESD Co., Tokyo
Personal computer for Windows95/98		NEC, Tokyo

polypropylene screen (8 × 8 clear strands per cm). By adjusting the number of sheets, I was able to control the appropriate amount of air introduced into the chambers; that is, the cool end wall was covered with three-, two-, or one-screen sheets from the ground to 0.75 m, 0.75 m to 1.7 m, and 1.7 m away from the top, respectively. This fine adjustment succeeded in preventing the reversal phenomenon often found in former TGC experiments in which the air temperatures near the air outlet were lower than those of the air inlet; this reversal was caused by the counter-flow of warmed air (e.g. Okada *et al.*, 1995).

At the side of both chambers, I built an additional Control Chamber (CC), 5 m long, 3 m wide, and 2.5 m high, to obtain enough space for the Control plot which was under ambient temperature and CO_2 conditions. The roof and the upper part of walls were also covered with 0.15 mm thick UV-transparent polyvinyl films, and the lower part was similarly covered with porous polypropylene screen to prevent the invasion of herbivorous insects and to circulate the outside air freely.

II-1-2. Creation of a temperature gradient

II-1-2-1. During the daytime with high solar radiation

The air in the chambers was naturally heated by incident solar radiation during the daytime. When the inside air was ventilated by a ventilator, an air temperature gradient was created along the long axis of the greenhouse in the daytime. The magnitude of the gradient depended on solar heat gain. The following equation theory to assess the temperature increase is derived from

chamber design (Okada, 1986).

$$\triangle T = H/(Cp\,\rho\,V + 0.5\,\alpha\,h_t) \quad (1)$$

Where $\triangle T$ is the air temperature difference between the air outlet and the inlet of the chamber (℃), H is sensible heat gain (W m^{-2} ≒ 0.20~0.35 S, S; solar radiation), Cp is specific heat of the air (=1004 J kg^{-1} $℃^{-1}$), ρ is density of the air (=1.2 kg m^{-3}), V is ventilation rate ($m^3\,m^{-2}\,sec^{-1}$), α is the ratio of the cover area (roof + walls) to the floor area, h_t is the heat transmission coefficient through cover (m^{-2} $℃^{-1}$). The factor 0.5 is given when the inside mean air temperature is assumed to be the average of the temperature at the air inlet and the outlet in the chamber. Equation (1) is expressed on a unit floor area basis. The solar radiation absorbed in the chamber is distributed to sensible heat convection, evapotranspiration and soil heat transfer. The values of these variables depended largely on the outside weather conditions as well as on the inside plants and floor conditions. In a conventional chamber the sensible gain (H) ranges from 20 to 35% of the external solar radiation (Okada, 1986). For plastic covered chambers, 6 W m^{-2} $℃^{-1}$ is a good approximation for the heat transmission coefficient (Okada and Takakura, 1981).

Equation (1) indicates the importance of ventilation rate (V) on the temperature gradient in the chamber. With appropriate ventilation controls it is possible to establish a rather stable temperature gradient in the chamber. In order to achieve the target temperature difference between the air inlet and 25 m, the ventilation rate was controlled according to the fluctuation of the air temperature caused by change in the incident solar radiation.

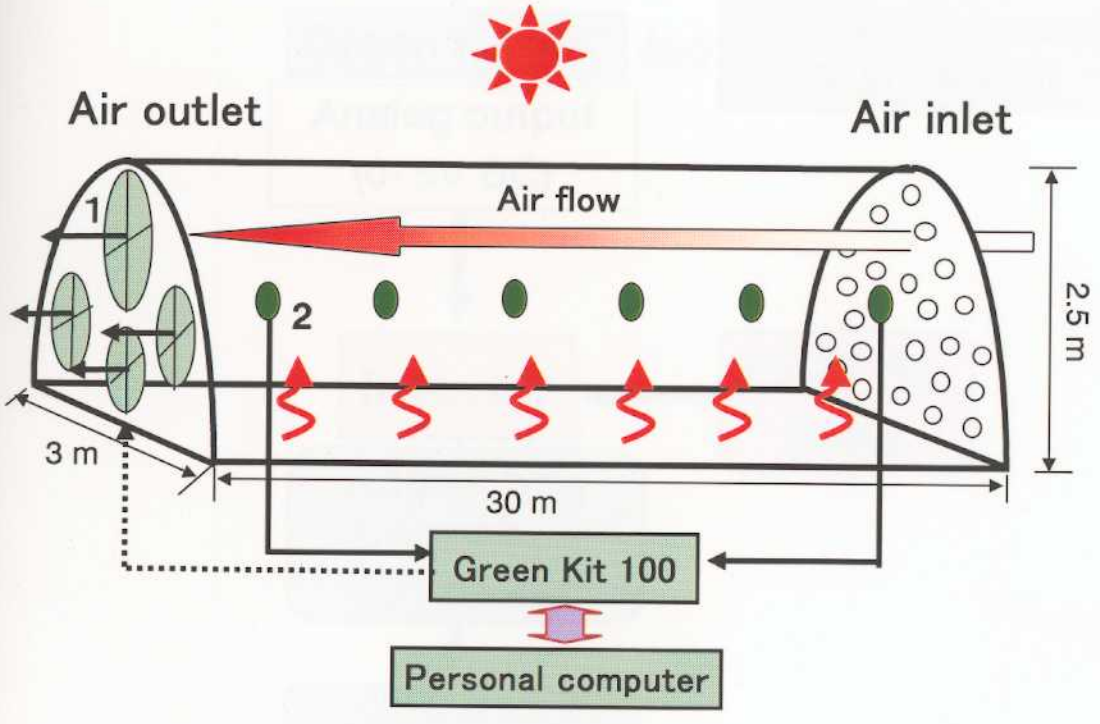

Figure 2. Schematic drawing of the creation of a temperature gradient in the daytime (high solar radiation). The ventilation rate depended primarily on the incident solar radiation in the chamber. Thermocouples were set on air inlet and every 5 m away from air inlet. 1, ventilator; 2, thermocouple.

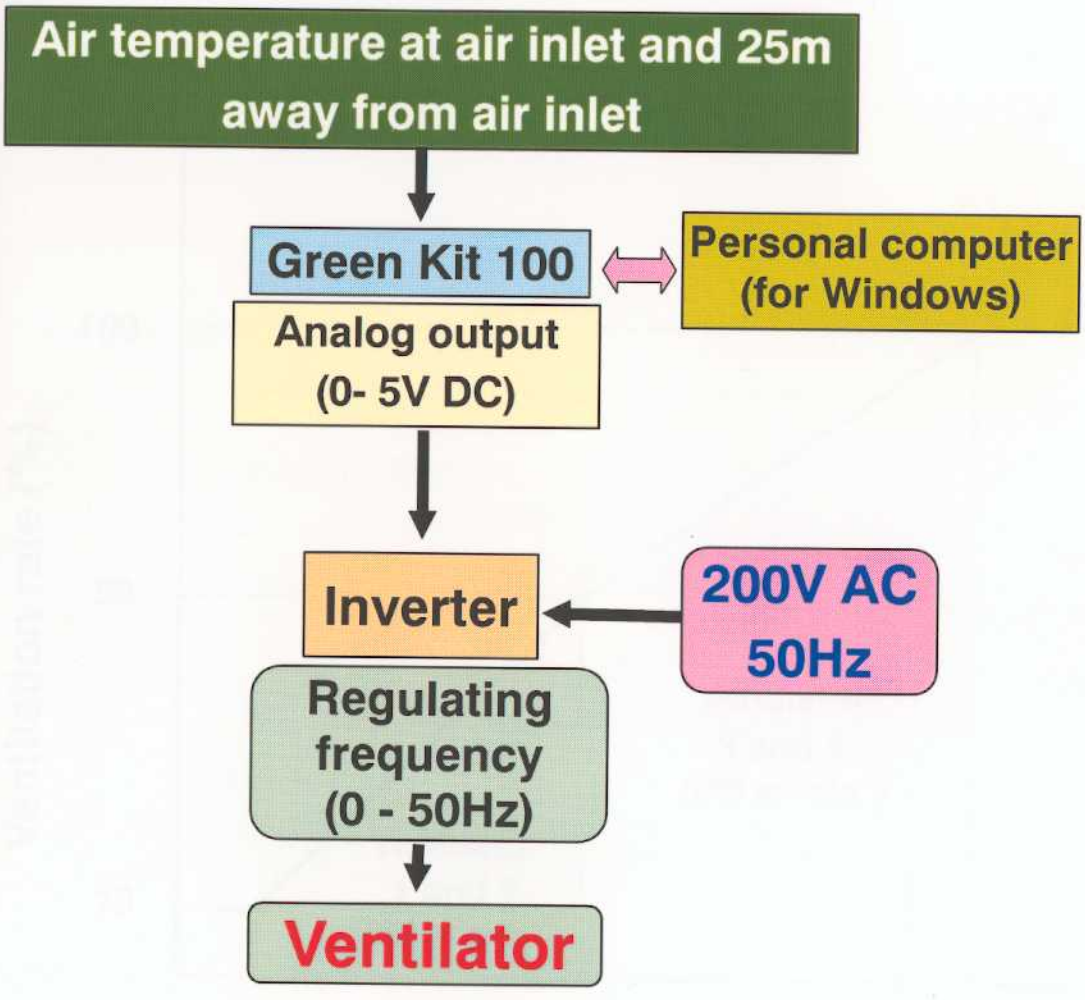

Figure 3. Schematic diagram of the ventilator control system.

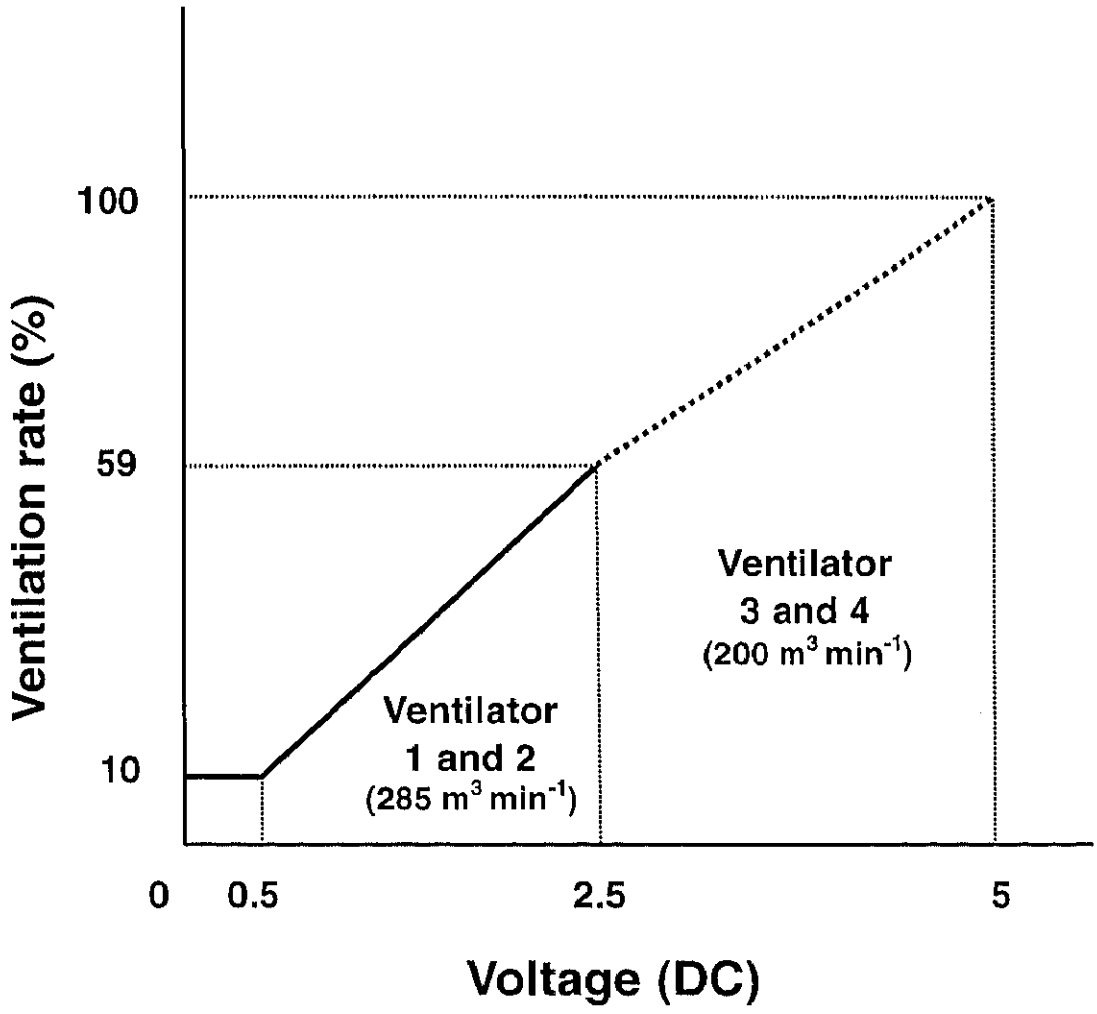

Figure 4. Schematic drawing of the relationship between the ventilation rate and the direct current signal from Green Kit 100.

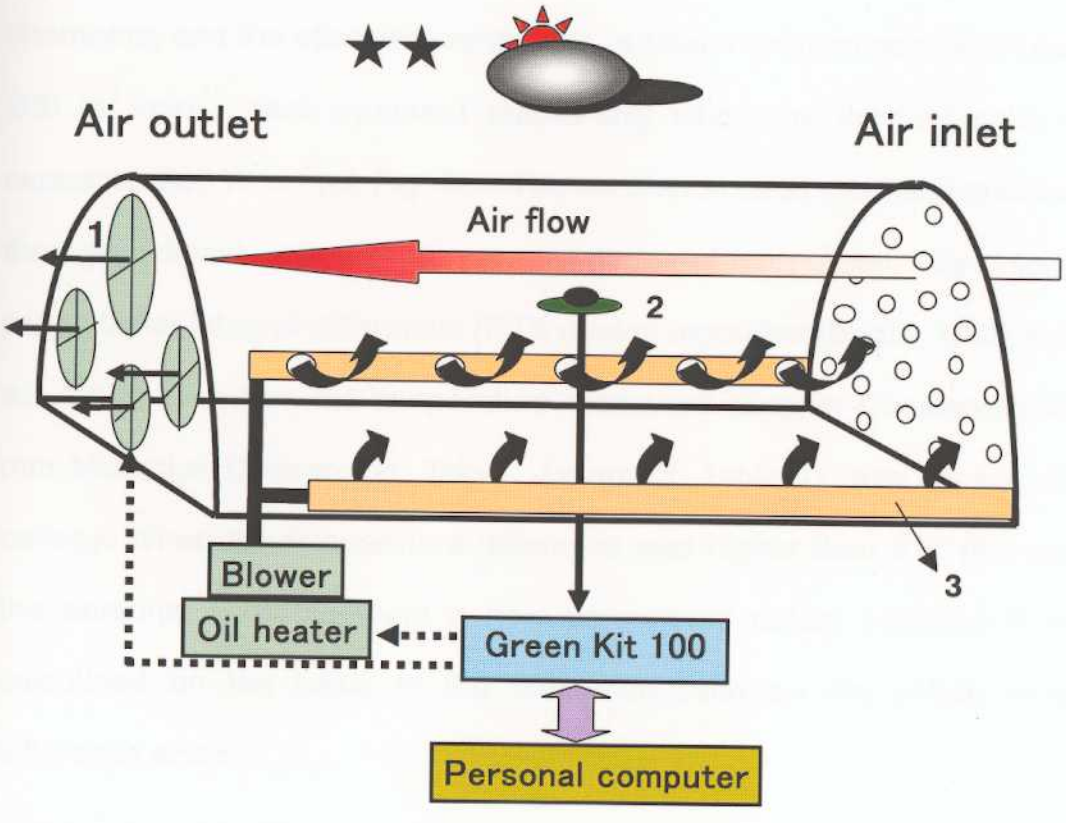

Figure 5. Schematic drawing of the creation of a temperature gradient in the nighttime (low solar radiation). The oil heaters were turned on when the incident solar radiation decreased below a set value of 180 to 220 W m^{-2}. 1, ventilator; 2, pyranometer; 3, warmed air injection pipe.

As shown in Fig. 2, four ventilators (FKVP404203 and 60607, Fulta Co. Japan; cf. Table 1) installed on the warm end wall were operated at 200AC voltage in proportion to the frequency (ranging from 0 to 50 Hz) of the inverter (cf. Fig. 3). As a rule, two of the ventilators (a total maximum ventilation capacity of 285 m^3 min^{-1}) were operated mainly to keep an optimum ventilation rate in the chambers, and the other two ventilators (a total maximum ventilation capacity of 200 m^3 min^{-1}) were operated additionally when the incident solar radiation exceeded 800 W m^{-2} (cf. Fig. 4). The ventilation rates were adjusted every 10-s through digital signals from a personal computer by applying a proportional-integral-differential (PID) control algorithm (Booth, 1993; Hendrey *et al.*, 1993) based on the temperature measured (Copper-Constantan wires, 0.3 mm Ninomiya Densen Co. Tokyo, Japan; cf. Table 1) from 10 cm above the canopy. When the temperature difference was higher than 5℃ (the set value), the personal computer sent a new percentage datum between 0 to 100%, calculated on the basis of the difference between the actual temperature difference and 5℃.

II-1-2-2. During the nighttime with low or no incident solar radiation

To maintain the temperature gradient at all times, I set an oil heater (EH-50N. Ennetsu. Gunma, Japan; cf. Table 1) which was fixed near each of the chambers. When the incident solar radiation measured by two pyranometers (MS-42, EKO. Tokyo, Japan; Table 1) decreased below a set value, the oil heater was automatically turned on. The warmed air was supplied through holes in one set of PVC pipes at each side in each chamber (cf. Fig. 5). The holes in

the PVC pipe were 0.5 cm diameter and placed at 50 cm intervals, approximately. The oil heaters were turned on when the incident solar radiation decreased below a set value of 180 to 220 W m^{-2} (e.g. it was higher in the growing season than in the juvenile season) because the rate of temperature rise depended on conditions such as the leaf area index of plant populations in the chambers. If the temperature difference between the air inlet and the outlet was in excess of the set point (5℃), the ventilation rate was automatically increased, or reduced if the difference was less than the set point. A minimum ventilation rate was set at 10% of the full rate to create the minimum directional airflow and to maintain it during the night or periods of low incident solar radiation, as might occur on a cloudy day.

II-1-3. Creation of a CO_2 concentration gradient in the CTGC

In order to create the desired CO_2 concentration gradient in the CTGC, CO_2 was injected at a rate controlled by automatically adjusting an electronic mass-flow controller (PI-D1-1, CDK Co. Nagoya, Japan; cf. Table 1).

As schematically demonstrated in the bottom of Fig. 6, the CTGC had an apparatus for CO_2 injection. This apparatus was composed of two sets of 15 CO_2 gas cylinders, a flow-direction changer, a gas heater (ATM-2A, Yutaka Ltd. Tokyo, Japan; cf. Table 1), and an electronic mass-flow controller; theCO_2 gas supply system included a blower, injection pipes, and a CO_2 measuring system (LI-6262, LI-Cor. Lincoln, USA; cf. Table 1). Each of the 15 gas cylinders was filled with 30 kg of liquefied CO_2 (concentration of 99.98%), which is equivalent to 15, 000 l in gaseous form at standard temperature and pressure. The CO_2

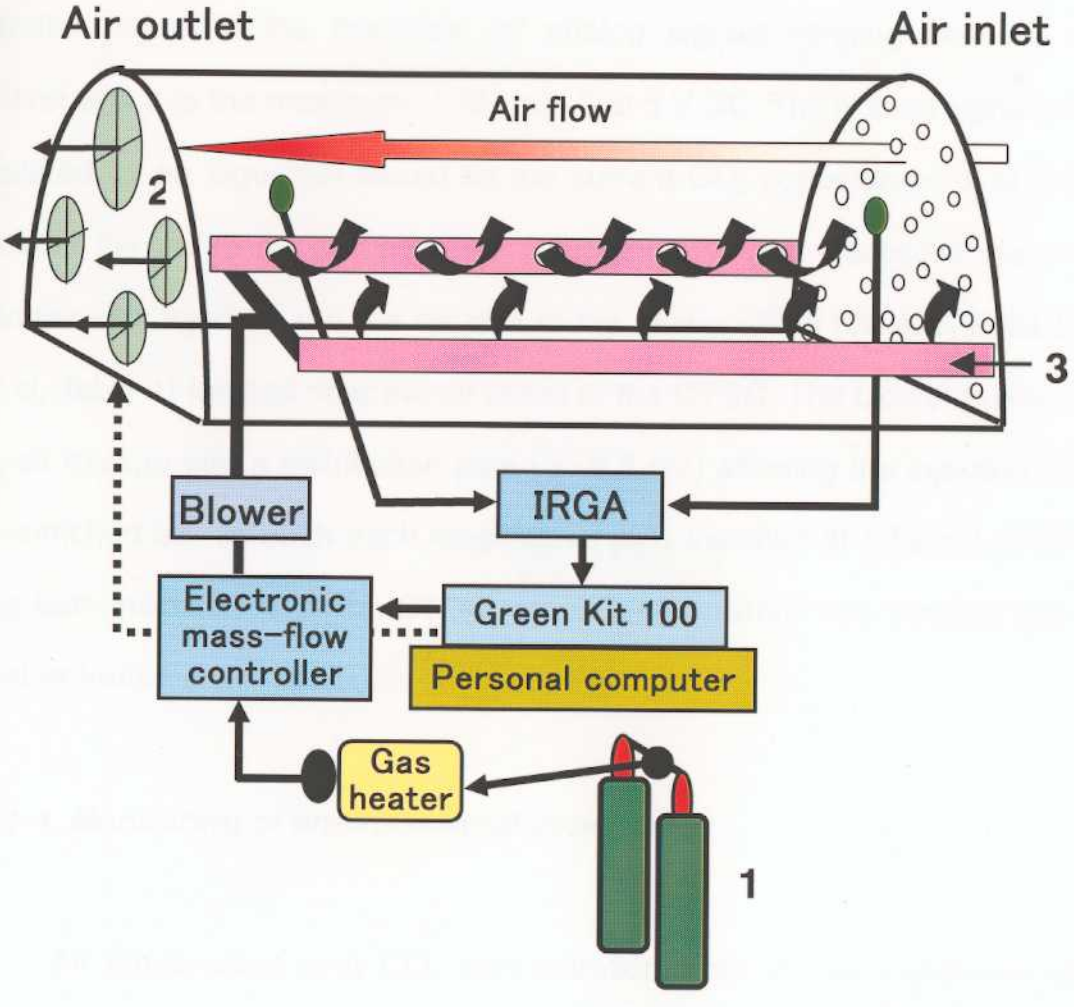

Figure 6. Schematic drawing of CO_2 gas supplying system in the CTGC. The system consists of CO_2 gas cylinder, gas heater, electronic mass-flow controller, blower, and injection pipe. 1, CO_2 gas cylinder; 2, ventilator; 3, CO_2 gas injection pipe.

gas flowed from one set of gas cylinders to an electronic mass-flow controller and then through a flow-direction changer, a pressure regulator, and a gas heater to prevent freezing due to adiabatic expansion. The electronic mass-flow controller regulated the flow rate by analog signals ranging from no CO_2 injection at 0 V to the maximum (100 l min^{-1}) at 5 V DC. The analog signals were calculated by an algorithm based on the current CO_2 concentrations at the air inlet and the outlet every 10-s. The CO_2 gas from the electronic mass-flow controller was injected into the air inlet of the blower (BLW100-401, Fulta Elec. Co.; cf. Table 1) located near the air outlet of the CTGC. The blower pushed the CO_2-air mixture into a distribution pipe (ϕ 5.5 cm) allowing the injection of the CO_2-enriched air. Through each longitudinal pipe installed at a height of 70 cm along both inside walls of the CTGC, the CO_2-air mixture was injected into the chamber from the air inlet to the outlet (cf. Fig. 6).

II-1-4. Monitoring of environmental conditions

All temperature and CO_2 concentration data in each chamber were monitored individually every 10-s and averaged over 5-min intervals. The controller/data logger system, Green Kit 100 (ESD Co., Tokyo, Japan; cf. Table 1), was operated by the DL300 software (ESD Co.; cf. Table 1) under Windows 95/98. This system is simple to use, even if there is no knowledge of technical programming.

II-2. RESULTS

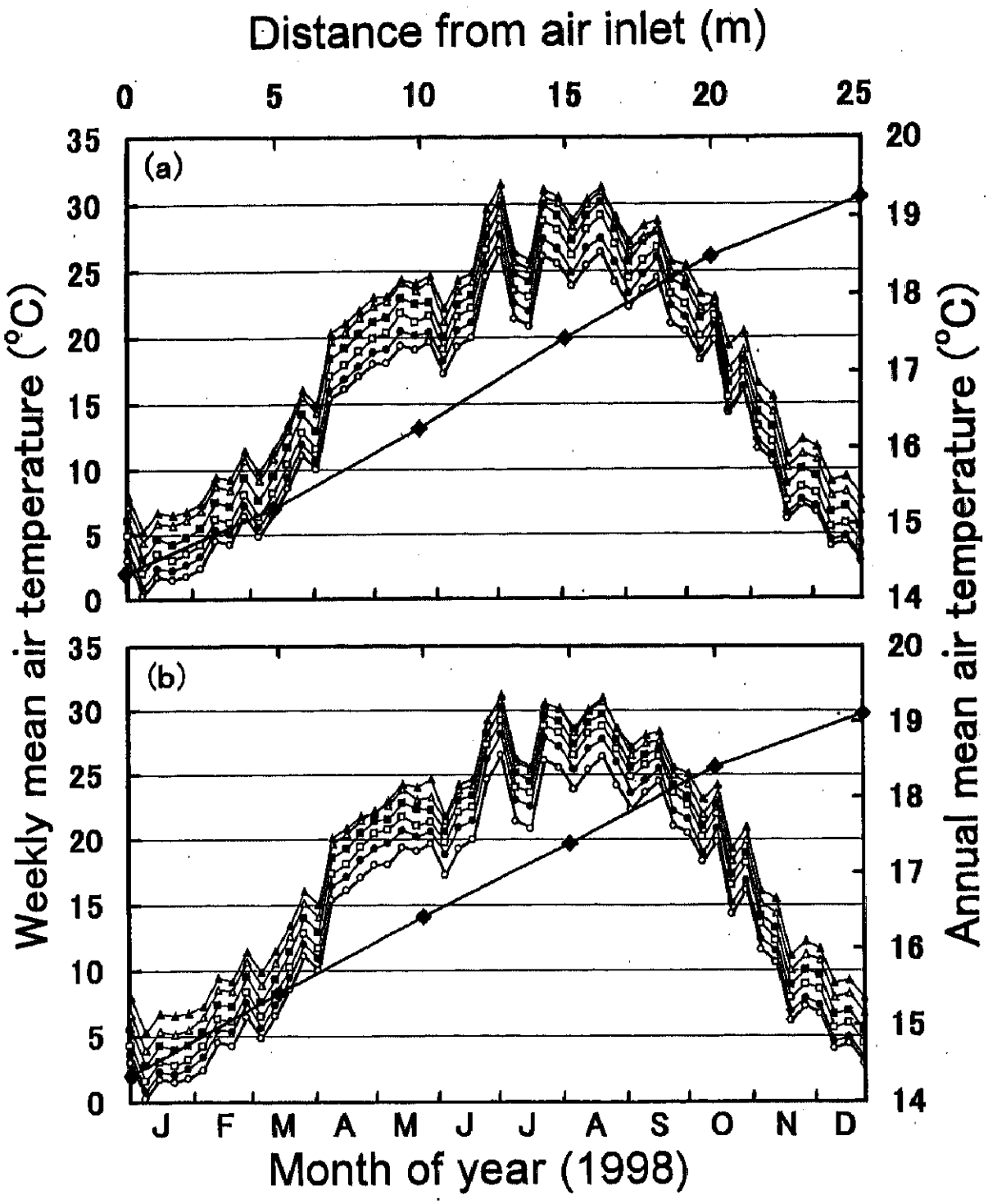

Figure 7. Annual changes in the weekly mean air temperature at every 5 m away from the air inlet in (a) the TGC and (b) the CTGC. Annual mean air temperature is also indicated by the closed diamond (plotted on the right ordinate). Symbols: open circles, ambient; closed circles, 5 m; open squares, 10 m; closed squares, 15 m; open triangles,20 m; closed triangles, 25 m away from the air inlet.

Figure 8. Diurnal courses of half-hourly mean air temperature at every 5 m away from the air inlet for four seasons in the TGC (left) and the CTGC (right). Those of winter (a and b, 10 Jan.), spring (c and d, 19 Apr.), summer (e and f, 3 July) and autumn (g and h, 12 Oct.) are, respectively, illustrated at top, upper middle, lower middle and at the bottom. Symbols: open circles, ambient; closed circles, 5 m; open squares, 10 m; closed squares, 15 m; open triangles, 20 m; closed triangles, 25 m from the air inlet. Daily mean air temperature is described in the box.

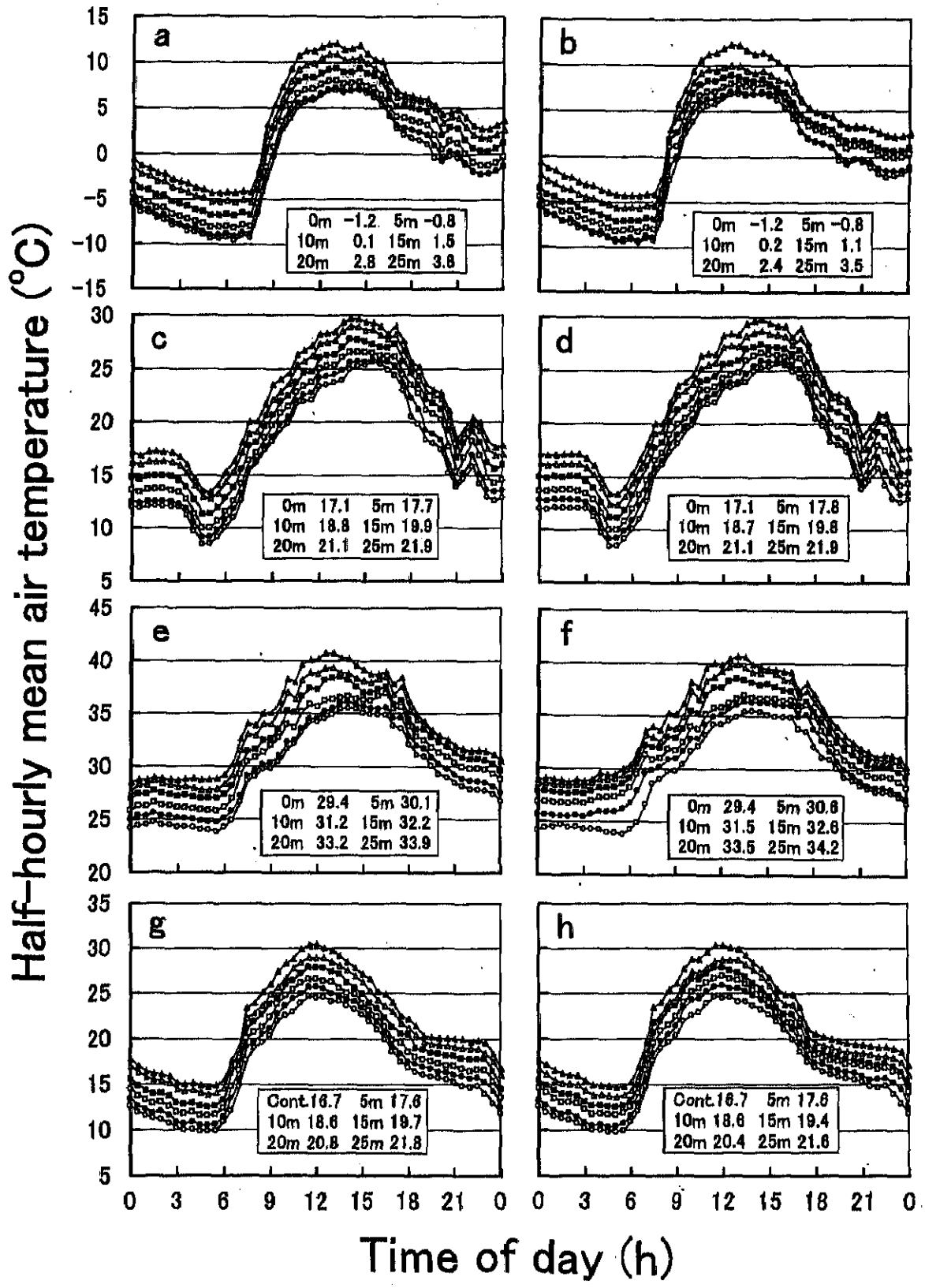
a
0m -1.2 5m -0.8
10m 0.1 15m 1.5
20m 2.8 25m 3.8
b
0m -1.2 5m -0.8
10m 0.2 15m 1.1
20m 2.4 25m 3.5
c
0m 17.1 5m 17.7
10m 18.8 15m 19.9
20m 21.1 25m 21.9
d
0m 17.1 5m 17.8
10m 18.7 15m 19.8
20m 21.1 25m 21.9
e
0m 29.4 5m 30.1
10m 31.2 15m 32.2
20m 33.2 25m 33.9
f
0m 29.4 5m 30.8
10m 31.5 15m 32.6
20m 33.5 25m 34.2
g
Cont.16.7 5m 17.6
10m 18.6 15m 19.7
20m 20.8 25m 21.8
h
Cont.16.7 5m 17.8
10m 18.6 15m 19.4
20m 20.4 25m 21.6
Half-hourly mean air temperature (°C)
Time of day (h)
0 3 6 9 12 15 18 21 0

II-2-1. Temperature gradient in both chambers

The air temperature gradients in both chambers increased linearly and were tested throughout 1998 (cf. Figs. 7a and b). The lowest and the highest weekly mean air temperature at the air inlet were 0.3℃ in mid-January and 26.5℃ in early July, respectively; at 25 m away from the air inlet, they were 5.3 and 31.5℃ in the TGC and, 5.3 and 31.2℃ in the CTGC. The air temperature at the air inlet exceeded 23.0℃ from July to September except for the last week of July when they abruptly fell to 20.9℃. From September onward in 1998 the air temperature fell gradually.

Annual mean air temperature (y-axis of the right-hand side; drawn with filled squares in Fig. 7) almost linearly increased from 14.3℃ at the air inlet to 19.2℃ at 25 m in the TGC, and from 14.3℃ at the air inlet to 19.1℃ at 25 m in the CTGC, respectively. Consequently, the warming of 1℃ every 5 m was satisfactorily realized with a precision of ±0.2℃ in both chambers. Air temperature was successfully regulated throughout all seasons in both chambers, even to the precision of each half hour (cf. Fig. 8).

Global warming conditions were well simulated for all plots in both chambers, independent of great seasonal and daily variations of ambient air, temperature and incident solar radiation.

II-2-2. CO_2 concentration gradient in the TGC and CTGC

The doubled CO_2 condition was at 25 m in the CTGC after 10 Feb., when the maximum CO_2 supply capacity was readjusted to be higher than the

demand (cf. Fig. 9). As a consequence, the mean CO_2 concentration at 25 m away from the air inlet was increased up to 799 ppm with a standard deviation of 7.9 ppm. This condition was maintained throughout all seasons, irrespective of the growth stage of the plants in the CTGC.

During the hot season from 22 June to 26 Sept. 1998, the mean CO_2 concentrations during the daytime (6:00-18:00) at 0, 10, and 25 m away from the air inlet in the CTGC were 372, 537 (1.4x), and 756 ppm (2x), respectively (cf. Fig. 10). However, CO_2 concentrations were higher than the desired concentrations during the nighttime (18:00-6:00). The nighttime CO_2 concentrations were not always constant even in the TGC, but were higher nearer the air outlet. The half-hourly mean CO_2 concentrations in the CTGC were finely regulated according to the diurnal change of the ambient CO_2 concentrations. In the TGC, there were no substantial differences among the daytime CO_2 concentrations monitored at 0, 10, and 25 m away from the air inlet. During the nighttime, on the other hand, the CO_2 concentrations were higher at 25 m away from the air inlet even in the TGC, due to the gradual accumulation of respiratory CO_2 from the plants and soil.

The daily trends of CO_2 concentrations (cf. Fig. 11) were maintained during all seasons, independent of the great daily and seasonal changes of ambient meteorological conditions such as incident solar radiation, air temperature, humidity, wind speed, and CO_2 concentration.

II-2-3. Moisture condition

The mean vapor pressures were higher far from the air inlet in the

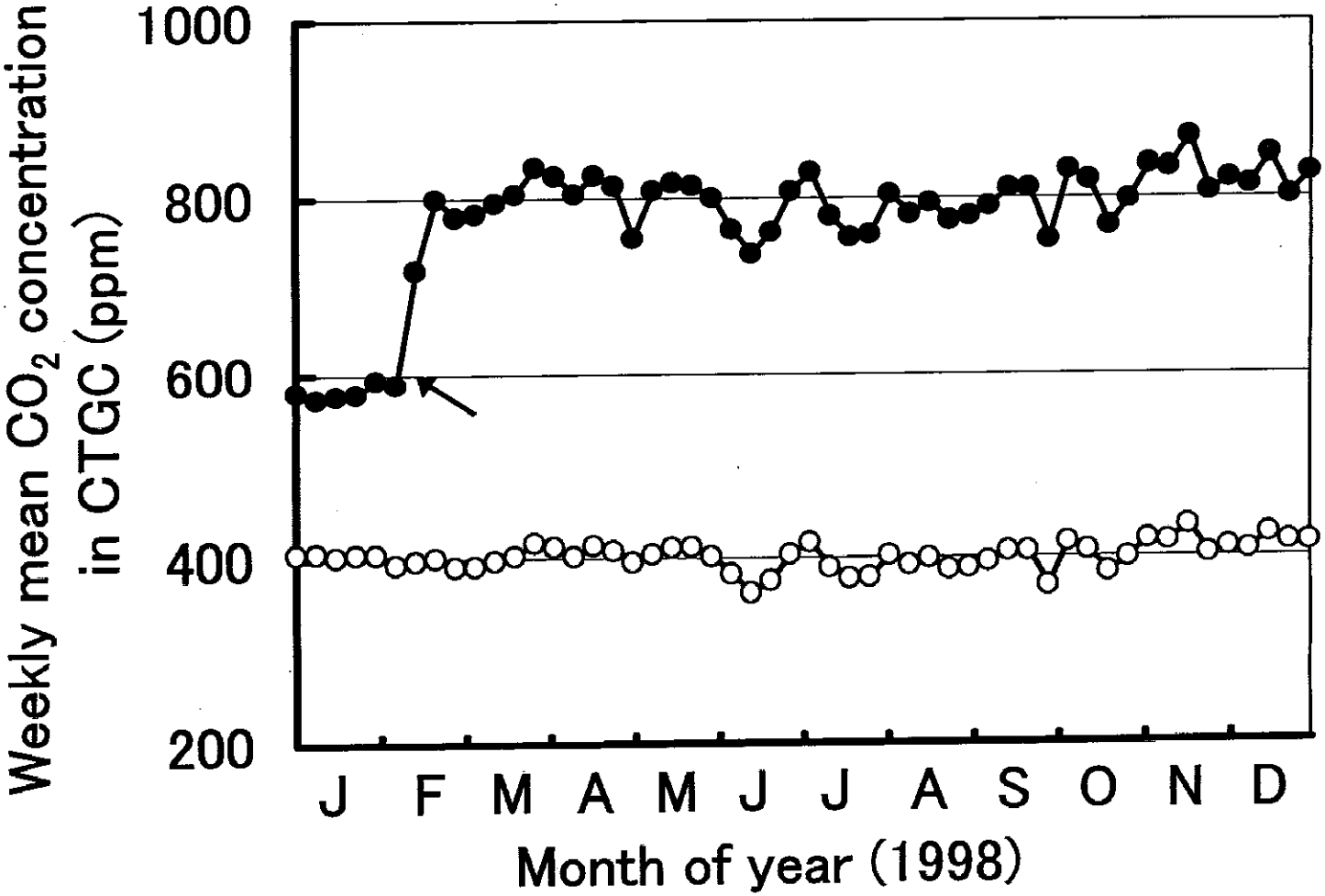

Figure 9. Annual changes of weekly mean CO_2 concentration at the air inlet (open circles) and 25 m away from the air inlet (closed circles) in the CTGC. Arrow indicates that the maximum CO_2 supply capacity was readjusted on 10 Feb. 1998.

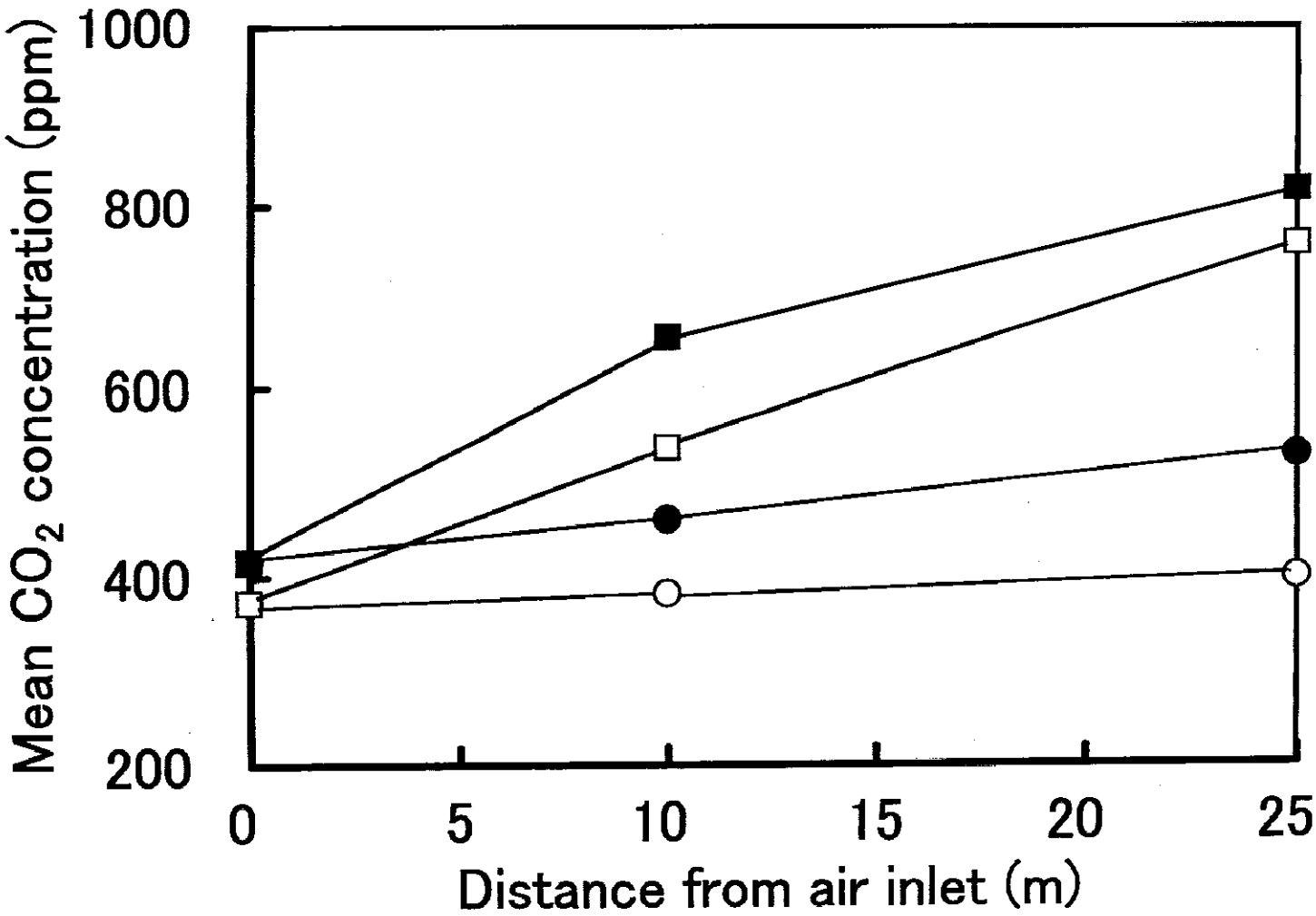

Figure 10. Mean CO_2 concentrations in the active growing season from 22 June to 26 Sept. are shown at 0, 10 and 25 m away from the air inlet in both chambers. Those of open and filled symbols indicate daytime (6:00-18:00; open circles, TGC; open squares, CTGC) and nighttime (18:00-06:00; closed circles, TGC; closed squares, CTGC) values, respectively.

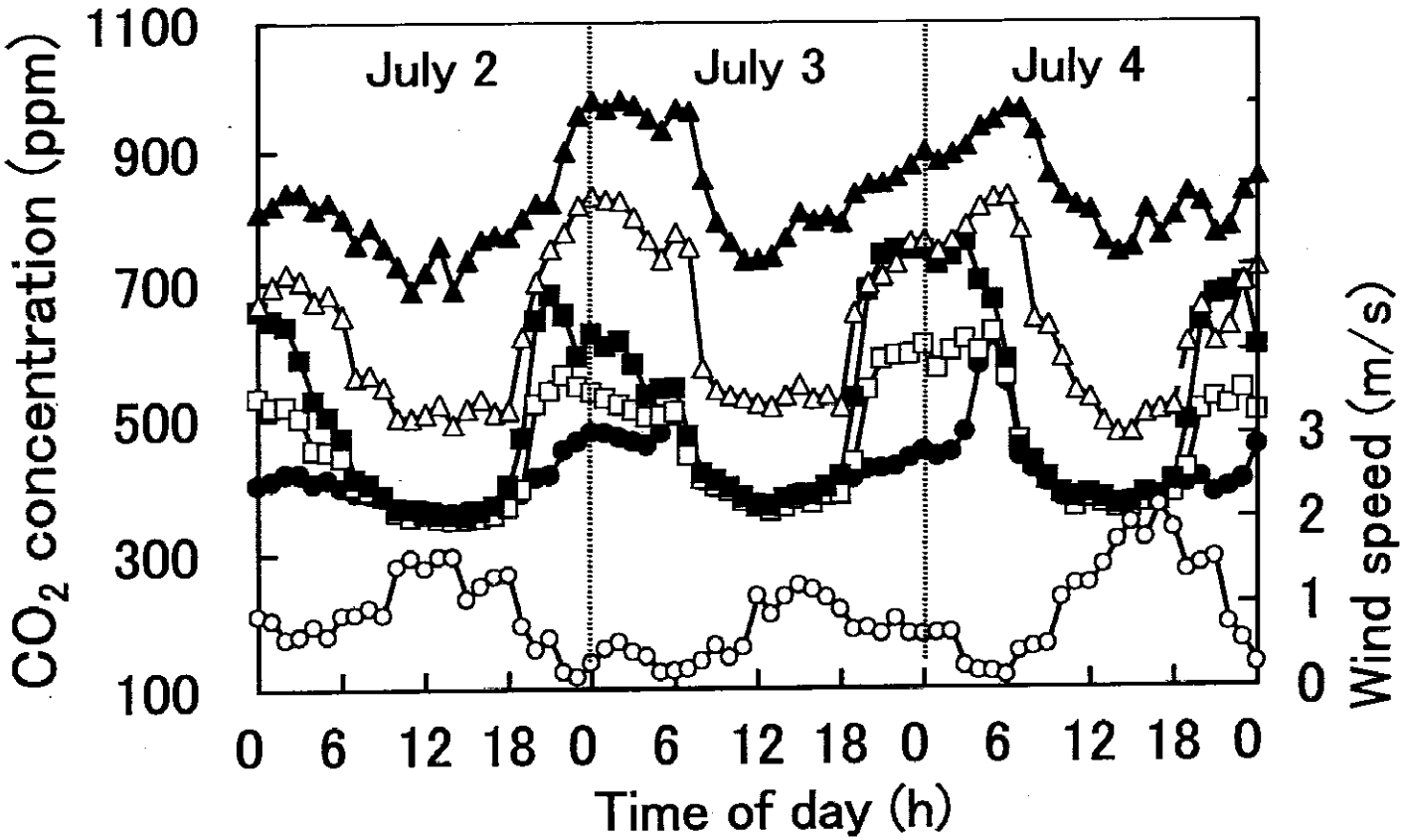

Figure 11. Diurnal courses of half-hourly mean CO_2 concentrations in both chambers compared with ambient CO_2 concentrations. Those were measured on July 2-4 at 10 and 25 m away from the air inlet. Symbols: open circles, wind speed in the TGC; closed circles, ambient; open squares, 10 m away from the air inlet in the TGC, closed squares, 25 m away from the air inlet in the TGC; open triangles, 10 m away from the air inlet in the CTGC; closed triangles, 25 m away from the air inlet in the CTGC.

daytime (6:00-18:00) and the nighttime (18:00-6:00) in both chambers (cf. Fig. 12). The vapor pressure deficits (VPD) were larger, especially in the daytime. The VPDs in both chambers were much higher during the daytime than at night. In contrast, during the nighttime the VPD was higher in the TGC than in the CTGC.

II-2-4. The relationship between incident solar radiation, ventilation rates and wind speed in both chambers

Wind direction in both chambers was always induced from the air inlet to the outlet by four ventilators. The relationship between the wind speeds and the ventilation rates were investigated before the growth experiment with material plants commenced. The wind speeds were measured with a hot-wire anemometer (Model 1000, Nihon Kagaku Co. Ltd., Tokyo, Japan) at heights of 0.4, 0.9, and 1.6 m above the ground at 5 m away from the air inlet in the CTGC. Wind increased from 15 to 60% of the full ventilation rate for every 5% increase of the ventilation rate (the total capacity of the four ventilators was 485 m^3 min^{-1}) (cf. Fig. 13). The wind speeds were highest at 0.9 m and lowest at 1.6 m among the three heights. Mean wind speeds in the three heights increased approximately linearly with the increasing percentage of the ventilation rate, having a gradient of 0.0097 m sec^{-1} per one percentage.

At full ventilation rate (=100%), the maximum wind speed was less than 1 m sec^{-1}. However, the actual maximum ventilation rate did not exceed 60% even around noon under a clear and hot summer weather condition.

The hourly changes in the ventilation rate were closely related to the

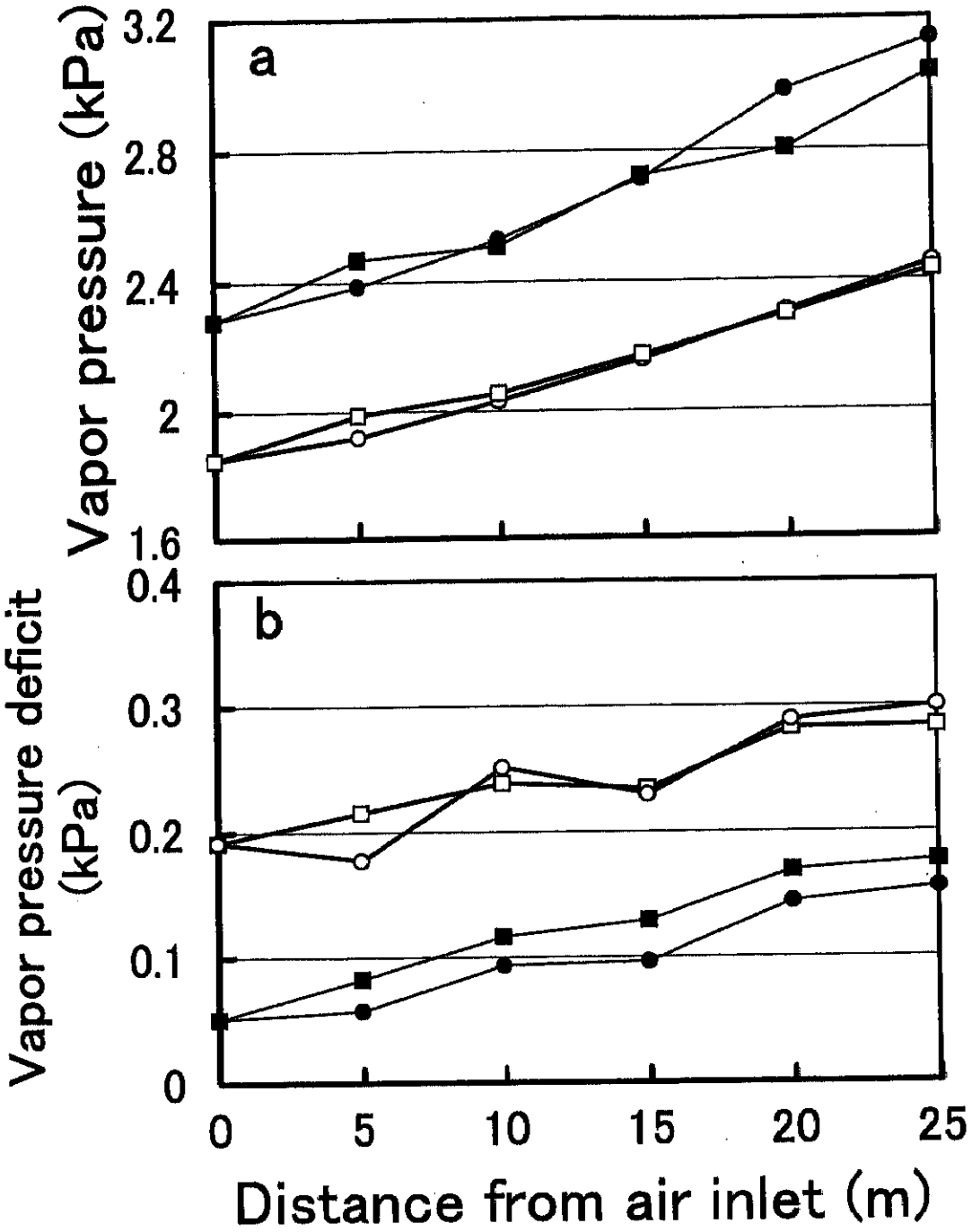

Figure 12. The means of vapor pressure (a) and vapor pressure deficit (b) during the active growing season from 27 May to 7 June, illustrated for every 5 m from the air inlet in both chambers at daytime and at nighttime. Symbols: open squares, TGC (daytime, 6:00-18:00); closed squares, TGC (nighttime, 18:00-06:00); open circles, CTGC (daytime); closed circles, CTGC (nighttime).

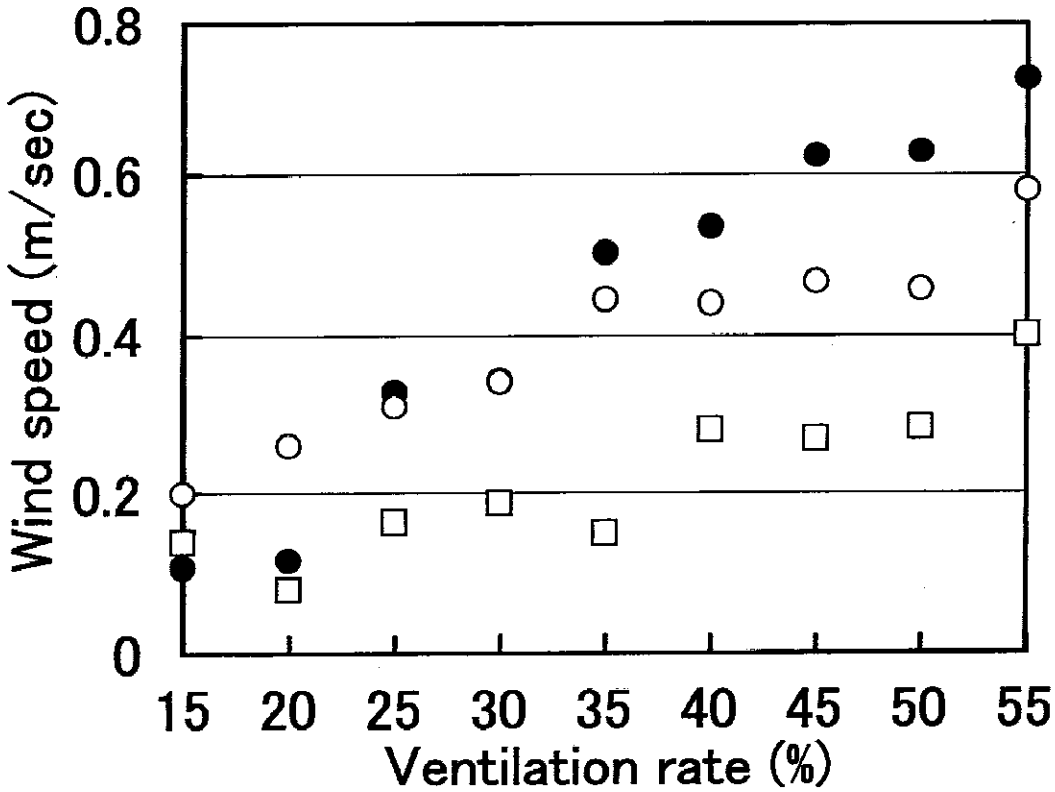

Figure 13. The relationship between ventilation rate and wind speeds measured in the CTGC. Right top is the relationship between ventilation rate and solar radiation indicating diurnal change of ventilation rate in the CTGC. Symbols: open circles, 40 cm above the ground; closed circles, 90 cm above the ground; open squares, 160 cm above the ground.

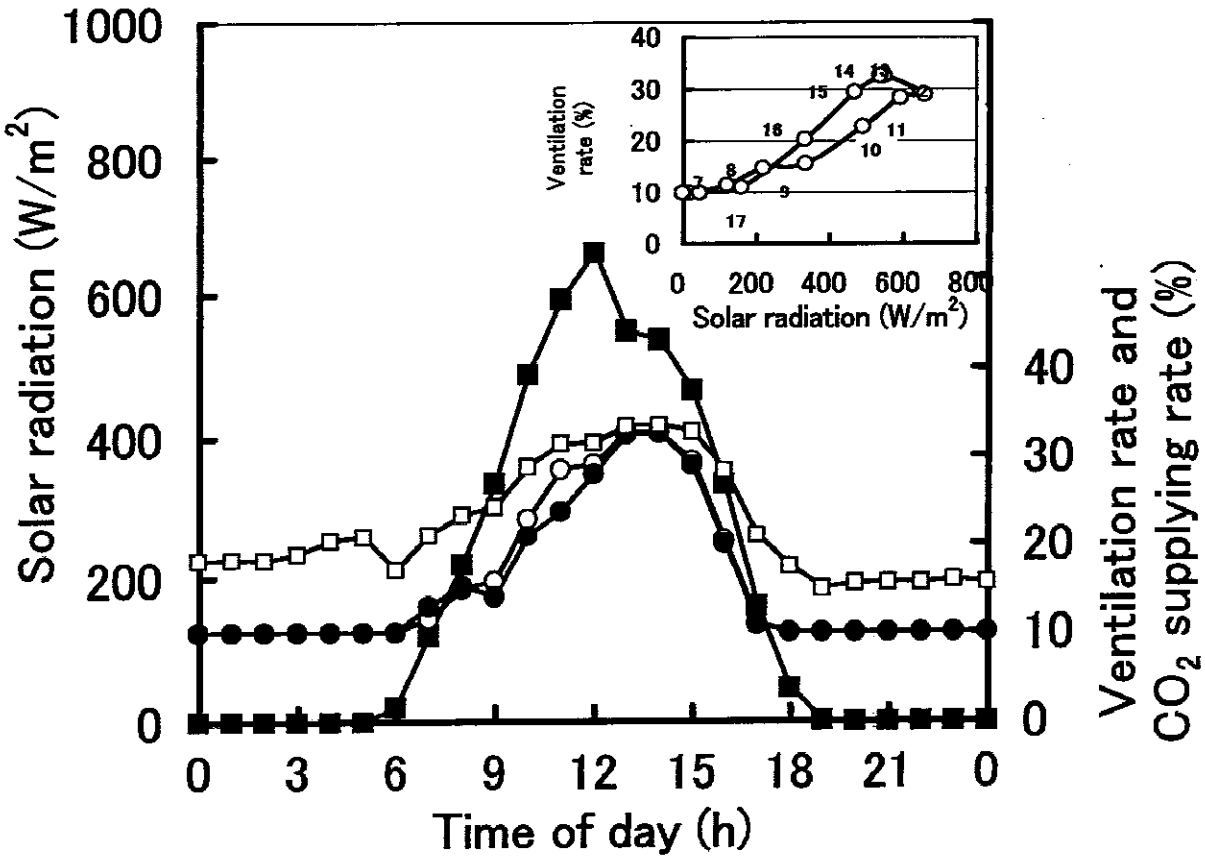

Figure 14. Ventilation rate in both chambers and daily changes of solar radiation and CO_2 release rate in the CTGC on a typical fine day (19 April, 1998). The relationship between the incident solar radiation and the ventilation rate in the CTGC in redrawn in the inlet. Symbols: closed circles, ventilation rate in the TGC; open circles, ventilation rate in the CTGC; closed squares, solar radiation; open squares, CO_2 release rate in the CTGC.

instantaneous incident solar radiation in both chambers (cf. Fig. 14) on a clear day when the maximum solar radiation exceeded 600 W m^{-2} around noon (19 April) and the maximum half-hourly mean air temperature was higher than 25℃ at the air inlet (cf. Fig. 7). However, incident solar radiation was not the only determinant of the ventilation rate. As shown in the inset of Fig. 14, the ventilation rates under the same incident solar radiation were always higher in the afternoon than in the morning.

II-2-5. Construction and operation costs

Construction costs were about \$92,000 (\$511 m^{-2}) for both chambers, and the annual operation costs were approximately \$43,400 (\$241 m^{-2}) in 1998 (\$20,000 for fuel and electricity for both chambers, and \$23,400 for CO_2 gas in the CTGC). To maintain the appropriate air temperature in both chambers (cf. Figs. 7 and 8), 15 tons of oil was consumed, mainly at night, which calculates to \$1,333 ton^{-1} for 24 h day^{-1} over 12 months in 1998. In addition, to maintain the appropriate CO_2 level in the CTGC (cf. Fig. 9), almost 14 tons of pure CO_2 was used to enrich 90 m^2 by an average of 190 ppm for 24 h day^{-1} over 12 months during 1998.